

Autosomal Recessive Ichthyosis with Hypotrichosis Caused by a Mutation in *ST14*, Encoding Type II Transmembrane Serine Protease Matriptase

Lina Basel-Vanagaite, Revital Attia, Akemi Ishida-Yamamoto, Limor Rainshtein, Dan Ben Amitai, Raziel Lurie, Metsada Pasmanik-Chor, Margarita Indelman, Alex Zvulunov, Shirley Saban, Nurit Magal, Eli Sprecher, and Mordechai Shohat

In this article, we describe a novel autosomal recessive ichthyosis with hypotrichosis syndrome, characterized by congenital ichthyosis associated with abnormal hair. Using homozygosity mapping, we mapped the disease locus to 11q24.3-q25. We screened the *ST14* gene, which encodes matriptase, since transplantation of skin from matriptase^{-/-}-knockout mice onto adult athymic nude mice has been shown elsewhere to result in an ichthyosislike phenotype associated with almost complete absence of erupted pelage hairs. Mutation analysis revealed a missense mutation, G827R, in the highly conserved peptidase S1–S6 domain. Marked skin hyperkeratosis due to impaired degradation of the stratum corneum corneodesmosomes was observed in the affected individuals, which suggests that matriptase plays a significant role in epidermal desquamation.

Autosomal recessive congenital ichthyoses are clinically and genetically heterogeneous genodermatoses characterized by abnormal epidermal differentiation. They can be classified into two groups: (i) primary ichthyoses limited to the skin and (ii) syndromic ichthyoses, associated with extracutaneous features.

Six genes are known to be associated with nonsyndromic autosomal recessive congenital ichthyoses: *TGM1* (MIM *190195),^{1,2} *ALOXE3* (MIM *607206), *ALOX12B* (MIM *603741),^{3,4} *ABCA12* (MIM *607800),^{5,6} *ICHTHYIN* (MIM +609383),⁷ and *FLJ39501*.⁸ In addition, linkage to chromosomal loci on 12p11.2-q13⁹ and 19p13.1-p13.2¹⁰ has been reported.

Several autosomal recessive ichthyoses with hair abnormalities have been described.¹¹ Netherton syndrome (NTS [MIM #256500]) is characterized by congenital ichthyosiform erythroderma, trichorrhexis invaginata, and atopic manifestations. Mutations in *SPINK5*, which encodes LEKTI, an inhibitor of serine proteases, were identified as the cause of NTS.¹² Congenital ichthyosis, follicular atrophoderma, hypotrichosis, and hypohidrosis syndrome (MIM 602400) is characterized by diffuse congenital ichthyosis, patchy follicular atrophoderma, generalized and diffuse nonscarring hypotrichosis, and marked hypohidrosis.^{13,14} Trichothiodystrophy with congenital ichthyosis—that is, ichthyosis, brittle hair, intellectual impairment, decreased fertility, and short stature (IBIDS [MIM

#601675])—a rare autosomal recessive disorder characterized by sulfur-deficient brittle hair and nails, mental retardation, impaired sexual development, and ichthyosis, is caused by mutations in the *ERCC3/XPB*¹⁵ and *ERCC2/XPD*¹⁶ genes. Ichthyosis, split hairs, and amino aciduria syndrome (MIM 242550) is characterized by lamellar ichthyosis, splitting of the hair shaft, amino aciduria, and mental retardation.¹⁷

In this study, we describe a novel autosomal recessive ichthyosis with hypotrichosis syndrome (ARIH) characterized by congenital ichthyosis associated with abnormal hair. We report on the identification of the disease-causing mutation in the *ST14* gene that encodes the serine protease matriptase.

Subjects and Methods

Patients

We ascertained a consanguineous Israeli-Arab family with ARIH, including three affected and five unaffected individuals. All the patients were siblings and were the offspring of parents who were first cousins. We obtained informed consent from all family members or their legal guardians, according to a protocol approved and reviewed by the National Committee for Genetic Studies, Israel Ministry of Health, and the Rabin Medical Center.

Homozygosity Mapping and Linkage Analysis

Genomic DNA for genotyping was extracted from leukocytes from peripheral venous blood in EDTA by standard procedures.¹⁸

From the Department of Medical Genetics (L.B.-V.; M.S.) and Pediatric Dermatology Unit (D.B.A.; R.L.; A.Z.), Schneider Children's Medical Center of Israel, Rabin Medical Center (L.B.-V.; M.S.), and Felsenstein Medical Research Center (R.A.; L.R.; N.M.; M.S.), Petah Tikva, Israel; Sackler Faculty of Medicine (L.B.-V.; M.S.) and Bioinformatics Unit, George S. Wise Faculty of Life Sciences (M.P.-C.), Tel Aviv University, Tel Aviv; Department of Dermatology, Asahikawa Medical College, Asahikawa, Japan (A.I.-Y.); Department of Dermatology and Laboratory of Molecular Dermatology, Rambam Health Care Campus (M.I.; E.S.), and Faculty of Medicine and Rappaport Institute for Research in the Medical Sciences, Technion–Israel Institute of Technology (E.S.), Haifa; and Microarray Facility, Department of Biological Services, Weizmann Institute of Science, Rehovot, Israel (S.S.)

Received November 10, 2006; accepted for publication January 8, 2007; electronically published January 23, 2007.

Address for correspondence and reprints: Dr. Lina Basel-Vanagaite, Department of Medical Genetics, Rabin Medical Center, Beilinson Campus, Petah Tikva, 49100, Israel. E-mail: basel@post.tau.ac.il

Am. J. Hum. Genet. 2007;80:467–477. © 2007 by The American Society of Human Genetics. All rights reserved. 0002-9297/2007/8003-0008\$15.00
DOI: 10.1086/512487

Table 1. Primers Used to Amplify the ST14 Gene

Primer Pair	Exon	Primer Sequence (5'→3')	
		Forward	Reverse
1	1	GAGGCCACACCTGAAACTA	GTGCCGGGAGTTGTACTTGA
2	1	GGTGATGGTGAGGGCCTTAG	GGTCTCACAGGCGTCGTC
3	1	AGCCGGAGAAAAGAGGAAGAG	ACAGGAAATTCACCTGTGC
4	1	GACGACGCTGTGAGACC	ACAGGAAATTCACCTGTGC
5	2	TTCTCCAAGCTGGACCTCAC	GGCCAAGAGATCCTCGTGA
6	3	AGTGATGGGAAGCAGTCAGG	GGTCCCTTTGCAGATCAC
7	4	ATGGGGGTGATCTGCAAAG	AGGACCTCCAGCACCATCT
8	5	GTGCTCTGGAGTCGCTCTG	GTCTTCTCTCTGGGGCACTG
9	5	GCCCATGTGTCCTGGAGT	GGCCAGCACGTAAGTCTTCTC
10	6	CAGTGCCCCAGAGAGAAGAC	GGCCTGGAAGATCGTCATA
11	7	AGGCTGAGGTCCACACC	TTGTACACCGTCACCAGGTC
12	7	CTTCCCTGACAGCCCTAC	GCGGCCAAGAGTCATAAACT
13	8	CTGTGGATGGGACCAGAGTT	TCTAGCCTGTGGCCTCCTAA
14	9	ACCTGCTGTGCAGCATCC	CATCTGCACAGGGAGACACA
15	10	AACAACACGCTGGGAGAAG	CCTCTCTCGCAGTATCTGG
16	11	GGAGGGTCCCACCAGAC	CAGCAAAGCACGATGCTAAC
17	12	CTGCTCCTGTGTGTTTGTGG	GGGCCAGAGGTCTTACACA
18	13	GGTCCCCAGGTAGCTCTGA	CTGGAGAGGCCACAGGACT
19	14	GAGCAGGGGTGCACTGAGT	GTCTGTCATGTGCGTGTG
20	15	GCCATTGGTGGTTTCTGG	ACCTCCAGGTGCACCCTCT
21	16	GGTCTCTGGCACACACTG	CCTCGGTGCCAACCTATC
22	17	ATCGTCTTCTCGTAGCAGCA	GTACTCTGCCGTTTCTCCA
23	17	CCACCCCTTCTCAATGACT	GACACGCAGAGGAAACACG
24	18	TCTGGGCTGTCCAGAGTTT	CACACCGCCTGGAAGAT
25	19	ATGTGGCTGGGCTTCTC	AGTCAGCGGTCCAGTCTCC
26	19	TTGGGACTGGATCAAAGAG	TTAGAGACAGGGGAGGCAGA
27	19	CAAAGTGGAGCTGGGAGGTA	CTCAGACCCGCTGTTTTCC
28	19	CCTCCTCAGTGAAGTGGTG	CTGACTCCAGGCTGTGCT

SNP genotyping was performed on Affymetrix Human Mapping 50k Xba 240 arrays. All procedures and methods were performed according to the manufacturer's instructions. In brief, for each sample, 250 ng of genomic DNA were digested using *Xba*I. Primer sequences were ligated to the digested fragments, and a single-primer PCR was performed on a PE9700 thermal cycler (Applied Biosystems). The PCR products were purified using Qiagen MinElute 96 UF plates. After purification, 40 µg of each amplified sample was fragmented, end-labeled, and hybridized to a GeneChip array. After washing and staining, the arrays were scanned using the GeneChip scanner 3000 with GeneChip Operating Software (GTYPE) version 1.4. Array CEL files were processed with GeneChip DNA Analysis Software version 4.0. For the examined samples, an average call rate of >95% was obtained.

Microsatellite markers were amplified by multiplex PCR, with use of standard protocols. Amplified markers were electrophoresed on an ABI 3700 DNA capillary sequencer and were analyzed with GENESCAN and GENOTYPER software (Applied Biosystems). For the LOD-score calculation, the two-point linkage analysis for markers *D11S4091*, *D11S4150*, and *D11S4131* on 11q24.3 was performed using the program SUPERLINK.¹⁹ We assumed a susceptibility allele with frequency 0.0001 and a recessive mode of inheritance with penetrance 0.99. For LOD-score calculations, the number of alleles was set as the number observed in the pedigree, rather than the number observed elsewhere, to provide a conservative estimate of the LOD score.

Sequencing of the Candidate Genes

Sequencing of the candidate genes was performed with primer sets designed using the Primer3 program. All exons—including

exon-intron junctions, 5' UTRs, and 3' UTRs—were amplified from genomic DNA with primers designed from the genomic sequences available from the University of California–Santa Cruz (UCSC) Genome Browser. Both strands of the PCR products were sequenced with BigDye Terminators (Applied Biosystems) on an ABI 3100 sequencer. Sequence chromatograms were analyzed using SeqScape software version 1.1 (Applied Biosystems). We initially tested one affected individual and one heterozygous parent.

Sequencing of the *ST14* gene was performed using 28 primer pairs (table 1). *ST14* mutation screening was performed on genomic DNA by PCR amplification with primer A, 5'-ATGTGCGTGGGCTTCTC-3' (forward), and primer B, 5'-AGTCAGCGGTCCAGTCTCC-3' (reverse), followed by sequencing.

Mutation Detection by Restriction Analysis

Amplification of a 379-bp fragment from genomic DNA was performed using primers A and B for 37 cycles at an annealing temperature of 55°C. The mutation introduces a *Bpm*I restriction site, which digests the 379-bp fragment into 215-bp and 164-bp fragments. The fragment was digested with 2 U/µg *Bpm*I (New England Biolabs), and the reaction products were separated by electrophoresis on 3% NuSieve/1% agarose gels.

Bioinformatics Methods

The gene and the protein were described using the UCSC Genome Browser (March 2006 assembly), the Ensembl Genome Browser (June 2006 assembly), and bioinformatics servers. To analyze conservation of the variation site, 10 vertebrate (from fish to human) sequence homologues to the human ST14 protein were collected using BLink ("BLAST Link"). Comparative sequence analysis (multiple sequence analysis [MSA]) was performed by ClustalW with a Java viewer (Clustal Alignment), as described by Higgins et al.²⁰ and Clamp et al.²¹ The ConSeq Server was used to validate sequence conservation and to predict functionality.²² The SIFT server sorts intolerant from tolerant amino acid substitutions and predicts phenotypic variations, as described by Ng and Henikoff.²³ Human ST14 protein was used as the input for SIFT analysis.

Immunohistochemistry

Formaldehyde-fixed 5-µm paraffin-embedded sections were treated with 3% H₂O₂ in methanol for 15 min at room temperature, were warmed in a microwave oven in citrate buffer for 15 min at 90°C, and were stained with antibodies directed against flaggrin (Novocastra), loricrin (Covance Research Products), involucrin (Covance Research Products), and cytokeratin 1 (BioGenex) or against preimmune rabbit antiserum for 1 h at room temperature. After extensive washings in PBS, the antibodies were revealed using the ABC technique (Zymed Laboratories), and the slides were counterstained using hematoxylin.

Electron Microscopy and Immunoelectron Microscopy

Postembedding electron microscopy with Lowicryl HM20 resin was performed as described elsewhere.²⁴ For immunoelectron microscopy, ultrathin sections were incubated with antibodies against LEKTI (Zymed Laboratories) and corneodesmosin (CDSN).²⁵

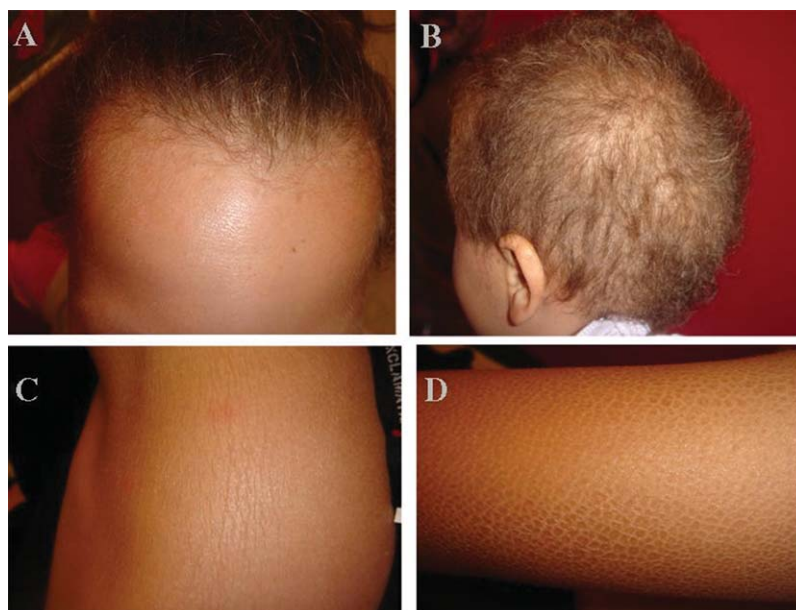


Figure 1. Clinical features of the patients. *A* and *B*, Hair of patients III-1 and III-8, respectively. Sparse and curly hair is observed. *C* and *D*, Ichthyotic skin of patient III-1 on the trunk and of patient III-5 on the upper limb, respectively.

Results

Clinical and Laboratory Evaluation

The patients were all born, after full-term, normal pregnancies, with normal birth weights. There was no colloid membrane. Ichthyosis and abnormal hair were present at birth. Patients III-5 and III-8 had a vernixlike layer covering the entire body, which was progressively shed during the first month of life. Hypotrichosis was generalized and diffuse (fig. 1*A* and 1*B*). Scaling was diffuse, including on the scalp, but the face was unaffected (fig.

1*A*, 1*C*, and 1*D*). Clinically, the hair of all the patients appeared curly, sparse, fragile, brittle, dry, and lusterless and showed slow growth. Light microscopy and scanning electron microscopy (SEM) examination of hair obtained from affected patients disclosed a number of abnormalities, including dysplastic hair (fig. 2*A* and 2*B*), pili torti (fig. 2*C*), pili bifurcati (fig. 2*D* and 2*E*), and central pili mono bifurcati (fig. 2*F*). Over time, scalp hair growth and appearance improved, and the scalp hair darkened with age. All three affected individuals had photophobia, and

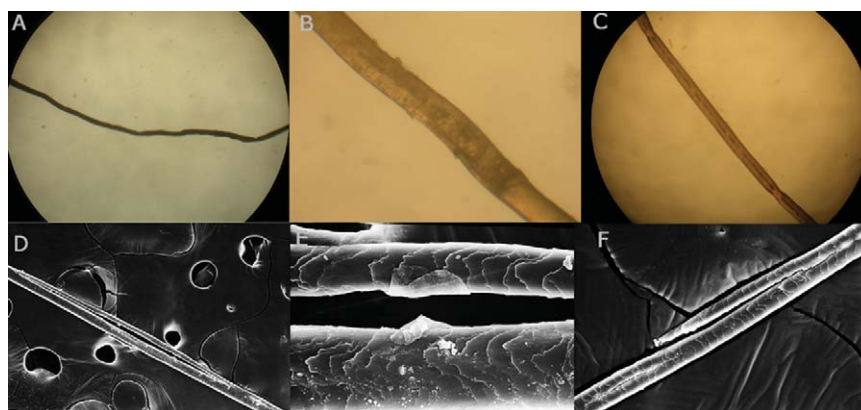


Figure 2. Light microscopy (*A–C*) and SEM (*D–F*) examination of hair obtained from affected patients. *A* and *B*, Dysplastic hair. Hair shafts are irregular, flaky, and undulating (*A*). *B*, Magnified undulation of panel *A*. *C*, Pili torti. Affected shaft is twisted on its own axis. *D* and *E*, Pili bifurcati. Each bifurcation produces two separate parallel branches that fuse again to form a single shaft; each branch is covered with its own cuticle. *F*, Central pili mono bifurcati: bifurcation that does not fuse again to the hair shaft and is located in the middle of the hair shaft. A minimum of 50 hairs from each patient were examined.

Table 2. Clinical Characteristics of the Patients

Characteristic	Patient		
	III-1	III-5	III-8
Age (in years)	17	8	2.5
Skin:			
Abnormalities at birth	Scaling	Vernixlike	Vernixlike
Color	Gray	Gray and brown	Gray and brown
Hair:			
Scalp hair	Dark brown	Uneven length, light brown	Uneven length, light brown
Eyebrows	Sparse and curly	Sparse, more lateral parts, light colored	Sparse, more lateral parts, light colored
Body hair	Sparse	Sparse	Sparse
Eyes:			
Corneal abnormality	No	No	Corneal opacity
Photophobia	Yes	Yes	Yes
Other	Pingueculum from age 11 years		
Other:			
Teeth	Normal	Notching, pitting	Conical primary teeth
Infections	No	Chronic sinusitis	No
Itching	Yes	Yes	Yes

NOTE.—All patients had skin abnormalities of the scalp, neck, abdomen, back, and limbs (extensor surfaces) and had long, curly, dark upper eyelashes and curly, sparse, fragile, brittle, dry, lusterless scalp hair, with receding frontal hairline.

one had corneal opacities. The clinical features of the patients are summarized in table 2.

Follicular atrophoderma, palmoplantar keratoderma, and hyperlinearity were not seen. The nails and mucosa were normal. No erythroderma, cardiac abnormalities, digital contractures, loss of pulp volume, ectropion, or hypoplasia of the nasal/auricular cartilage was observed. Sweating was normal, and there were no episodes of hypernatremic dehydration or hyperthermia. There were no atopic manifestations or photosensitivity. Complete blood count, urea, creatinine, liver enzymes, T-cell count, and immunoglobulins IgG, IgM, IgA, and IgE were all normal.

Patients III-2, III-3, III-6, and III-8 also have Hirschsprung disease, which is unrelated to the ichthyosis. Patient III-2 died at age 2.5 years from gastrointestinal complications of severe Hirschsprung disease (total colonic aganglionosis).

ARIH Mapping on 11q24.3-q25

A visual inspection of the SNP data showed that all the patients exhibited a large continuous segment of homozygosity for 53 consecutive SNPs, encompassing 5 Mb between markers *rs3926407* and *rs576825* on 11q24.3-q25 (table 3 and our tab-delimited txt file [online only]). These data were supportive of homozygosity by descent. Other, smaller genomic regions showing homozygosity in consecutive SNPs in all the patients on chromosomes 2, 5, 8, 9, 13, 14, and 17 were excluded by genotyping microsatellite markers *D2S2375*, *D2S2360*, *D5S1384*, *D5S1505*, *D8S549*, *D8S1731*, *D9S52*, *D9S104*, *D9S43*, *D9S251*, *D13S286*, *D13S1311*, *D13S173*, *D13S1265*, *D13S801*, *D14S592*, *D14S1429*, *D17S947*, *D17S917*, and *D17S808* in all nine family members (data not shown). Linkage to the locus on chromosome 11q24.3-q25 was confirmed by genotyping microsatellite markers *D11S4091*, *D11S4150*, and *D11S4131* in all nine family members (fig. 3A). LOD-score analysis for the marker *D11S4150* yielded a Z_{\max} score of

2.21 at recombination fraction (θ) 0.00 (table 4). A higher LOD score could not be obtained because of the small family size. The candidate region contains 22 known or predicted genes (fig. 3B).

Mutation Analysis

All exons—including promoter region, exon-intron junctions, and 5' and 3' UTRs—of the *BARX2* gene were sequenced, and no pathogenic sequence changes were found. *BARX2*-knockout mice display short hair.²⁶

Sequencing of the *ST14* gene revealed missense mutation c.2672G→A in exon 19 (according to “Recommendations for the Description of DNA Sequence Variants” [Ensembl Genome Browser]) (fig. 3C). The mutation causes a glycine→arginine change at residue 827 (G827R) of the protein, in the peptidase S1–S6 domain.

The *ST14* mutation segregated with the disease; affected patients displayed homozygous mutations, whereas parents displayed heterozygosity for a normal and a disease allele, consistent with autosomal recessive inheritance (fig. 3A). The mutation was not observed in 434 chromosomes from unrelated control individuals of Arab origin.

MSA was performed using 10 protein-sequence homologues for human ST14, including vertebrates from fish to human. A highly conserved region is present at the C-terminal region of the protein, harboring the Tryp_SPC (trypsinlike serine protease) domain, which includes the G827 residue of the human protein (fig. 4A). The ConSeq Server was used to further support these data. The peptidase C-terminal domain is shown (fig. 4B). Predicted results for residue G827 in the human protein showed that no change in this amino acid is tolerated (results not shown). Structural analysis of matriptase (1EAW in the Protein Data Bank) showed that the G827 variation is only two residues away from an important catalytic residue (serine 825).

Table 3. Homozygosity for SNP Markers on 11q24.2-q25

Chromosome and Location	SNP	Genotype for Patient		
		III-1	III-5	III-8
11q24.2:				
126135641	rs2226935	BB	BB	BB
126153350	rs1946052	AA	AA	AA
126259661	rs1940007	BB	BB	BB
126259725	rs1940006	AA	AA	AA
126314224	rs1939990	AA	AA	AA
126314287	rs1939991	BB	BB	BB
126314915	rs1939992	AA	AA	AA
126357648	rs631562	AA	AA	AA
126369604	rs488054	BB	BB	BB
126369798	rs541783	BB	BB	BB
126397423	rs1944627	AA	AA	AA
126401733	rs642387	AA	AA	AA
126402187	rs503397	BB	BB	BB
126553569	rs1944828	BB	BB	BB
126553743	rs1944827	BB	BB	BB
126861051	rs749514	AA	AA	AA
126861482	rs1729076	AA	AA	AA
126936044	rs356248	BB	BB	BB
126944448	rs356262	BB	BB	BB
126971973	rs763300	BB	BB	BB
127004821	rs10490847	BB	BB	BB
127004961	rs7928097	AA	AA	AA
11q24.3:				
127344152	rs1364780	AA	AA	AA
127525578	rs1477577	AA	AA	AA
127562693	rs476994	AA	AA	AA
127584911	rs1940356	AA	AA	AA
127585108	rs1940357	BB	BB	BB
127653338	rs510628	AA	AA	AA
127654275	rs722345	BB	BB	BB
127774235	rs2323123	BB	BB	BB
127920339	rs4128561	AA	AA	AA
127921152	rs4129229	BB	BB	BB
128134145	rs631647	AA	AA	AA
128134871	rs670809	BB	BB	BB
128416643	rs2155177	BB	BB	BB
128466905	rs657820	BB	BB	BB
128624506	rs4129583	BB	BB	BB
128904021	rs2008849	AA	AA	AA
128983138	rs2172487	BB	BB	BB
128984385	rs1873873	BB	BB	BB
129012244	rs952131	BB	BB	BB
129513314	rs879780	BB	BB	BB
129860441	rs3898490	BB	BB	BB
11q25:				
129879261	rs1272496	BB	BB	BB
130306606	rs1893225	AA	AA	AA
130679085	rs1793584	BB	BB	BB
130680535	rs1114296	BB	BB	BB
130697593	rs1793783	BB	BB	BB
130729658	rs4128590	BB	BB	BB
130729798	rs4128594	AA	AA	AA
130853281	rs1355982	BB	BB	BB
130897898	rs411280	AA	AA	AA
131091392	rs796873	AA	AA	AA

NOTE.—SNPs are shown on the dbSNP Web site.

Consequences of G827R in ST14

Marked acanthosis and a much thickened stratum corneum were demonstrated in affected skin by light microscopy (fig. 5). Since it has been suggested that proteases in general and matriptase in particular play an important role in the formation of the epidermal barrier,²⁷ we compared the expression of a number of elements of the cornified cell envelope in skin-biopsy samples obtained from patients and healthy control individuals. No significant differences were noticed in the intensity or pattern of expression of filaggrin, loricrin, involucrin, and keratin 1 between unaffected and affected skin (fig. 5).

We then examined the ultrastructural consequences of the G827R mutation in the *ST14* gene. We first examined the granular layers of the epidermis from a patient. Lamellar granules and keratohyaline granules displayed normal features. Immunoelectron microscopic examination of the skin-biopsy samples of a patient revealed normal distribution of LEKTI and CDSN (fig. 6).

The most remarkable and consistent abnormal finding was the conspicuous presence of intact corneodesmosomes in the upper cornified layers of affected epidermis, in contrast with the normal degradation of these structures in control skin (fig. 7). This finding suggests a major physiological role for matriptase during epidermal desquamation.

Discussion

In this study, we describe a novel autosomal recessive ichthyosis syndrome featuring both ichthyosis and abnormal hair distribution and structure, which we have named “autosomal recessive ichthyosis with hypotrichosis syndrome.” This disorder is clinically distinct from other genodermatoses involving skin and hair abnormalities. Compared with subjects affected with NTS, our patients have a milder disease, no erythrodermatous skin changes, no atopic manifestations, and no increased IgE. Congenital ichthyosis, follicular atrophoderma, hypotrichosis, and hypohidrosis syndrome is distinguished by the presence of hypohidrosis and follicular atrophoderma, which were not observed in our family. The ichthyosis, split hairs, and amino aciduria syndrome is characterized by mental retardation, whereas our patients have intact cognition. Mental retardation, brittle nails, and impaired sexual development are present in trichothiodystrophy with congenital ichthyosis syndrome (Tay or IBIDS syndrome); these were absent in our patients. The syndrome of ichthyosis follicularis with atrichia and photophobia (IFAP syndrome [MIM %308205]) is characterized by severe follicular hyperkeratosis, complete baldness, and photophobia; however, our patients have no atrichia or ichthyosis follicularis. Most importantly, IFAP syndrome is considered an X-linked condition.²⁸

We have demonstrated that this new syndrome (i.e., ARIH) is caused by a mutation in *ST14* that encodes matriptase, a type II transmembrane serine protease of the

S1 trypsinlike family.²⁹ Taking into account strict protease domain conservation and residue-change properties, in addition to its critical location near an important catalytic residue (serine 825), we predict that the amino acid change G827R leads to a severe change in protein function. This protein contains an N-terminal transmembrane domain, two tandem repeats of a CUB (C1r/s, Uegf and bone morphogenetic protein-1) domain, four tandem repeats of a low-density lipoprotein receptor domain, and a conserved extracellular serine protease catalytic domain.³⁰ Matriptase is expressed predominately in the epithelial cells of the surface-lining epithelium.³¹ In the interfollicular epidermis, matriptase expression is restricted to the postmitotic transitional layer of keratinocytes undergoing terminal

Table 4. Two-Point LOD Scores for Chromosome 11q24 Markers

Locus	LOD at $\theta =$						
	.00	.01	.05	.10	.20	.30	.40
<i>D11S4091</i>	2.0047	1.9569	1.7651	1.5245	1.0425	.5725	.1736
<i>D11S4150</i>	2.2122	2.1657	1.9776	1.7382	1.2481	.7525	.2912
<i>D11S4131</i>	$-\infty$.1701	.6990	.7853	.6568	.4177	.1692

differentiation.³² Similar to some other members of the type II transmembrane serine-protease group, matriptase exists in a soluble and membrane-bound form.^{33,34} The activation of matriptase requires proteolytic cleavage that

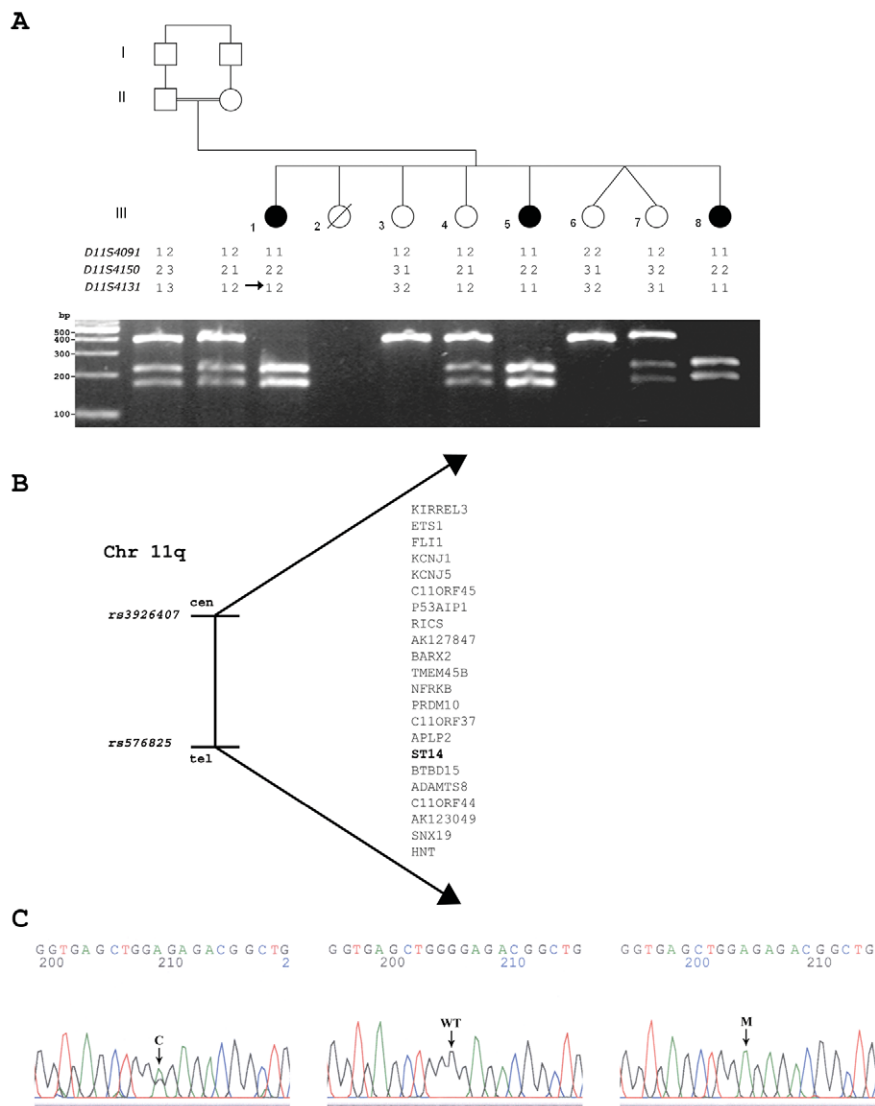


Figure 3. Family tree, candidate region, and mutation analysis. *A*, Pedigree of the family and segregation analysis of the mutation. Segregation was assayed by PCR amplification of the genomic DNA and restriction by *Bpm*I. The wild-type allele is uncut. Blackened symbols represent affected individuals. An arrow shows informative recombination. *B*, Candidate region. *C*, Mutation analysis of *ST14*. Sequence chromatogram from wild-type (WT), carrier (C), and affected (M) genotypes on genomic DNA.

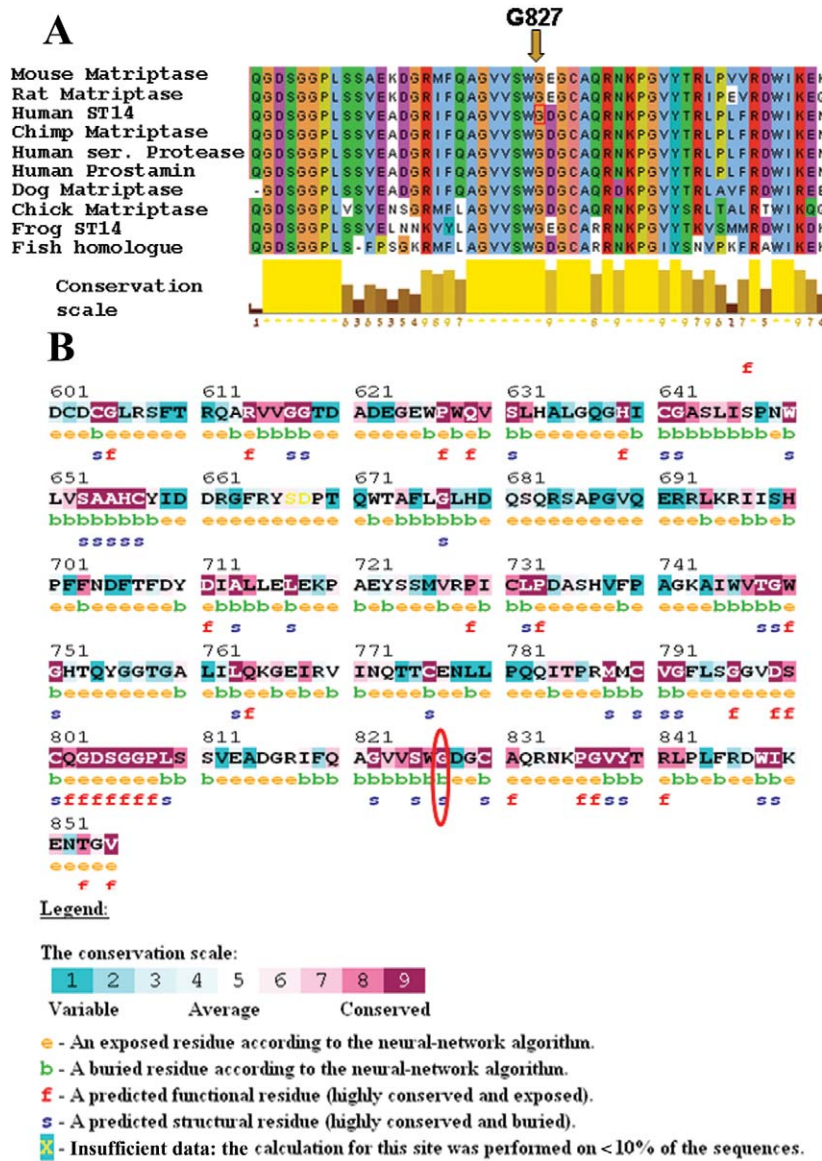


Figure 4. Multiple alignment and conservation analysis of human *ST14* with its orthologues. **A**, Multiple sequence alignment, performed by ClustalW (Clustal Alignment), with use of 10 protein sequences of matriptase, including vertebrates from fish to human: *Homo sapiens* (human) *ST14*, (GenBank accession number NP_068813), *Homo sapiens* (human) prostamin (GenBank accession number BAB20376), *Homo sapiens* (human) serine protease (GenBank accession number AAG15395), *Pan troglodytes* (chimpanzee) homologue (GenBank accession number XP_508863), *Mus musculus* (mouse) matriptase (GenBank accession number BAE38987), *Rattus norvegicus* (rat) matriptase (GenBank accession number AAH97271), *Gallus gallus* (chicken) matriptase (GenBank accession number XP_417872), *Canis familiaris* (dog) matriptase (GenBank accession number XP_546396), *Xenopus laevis* (frog) matriptase (GenBank accession number AAH71077), and *Danio rerio* (zebrafish) hypothetical protein (GenBank accession number NP_001035441). G827 is marked with an arrow. Residue colors represent amino acid biochemical properties according to Zappo colors. Conservation scale is shown below the alignment (yellow bars). **B**, Sequence conservation analysis, performed using the ConSeq Server, with internal MSA alignment serving as input. Residue G827 is circled in red. Conserved regions are marked with dark magenta, and variable regions are marked with green. Exposed (e) and functional (f) residues can be seen.

converts the enzyme from a one-chain zymogen to an active two-chain protease.³⁵ Several proteases and their inhibitors—such as cathepsin L, cathepsin D, cathepsin C, cystatin M/E, the stratum corneum chymotryptic enzyme (KLK7), the stratum cor-

neum tryptic enzyme (KLK5), and LEKTI—are important in epidermal homeostasis and/or hair follicle formation.³⁶ Two serine proteases of the kallikrein family—KLK7 and KLK5—have been implicated in the degradation of corneodesmosomal proteins in the epidermis.³⁷

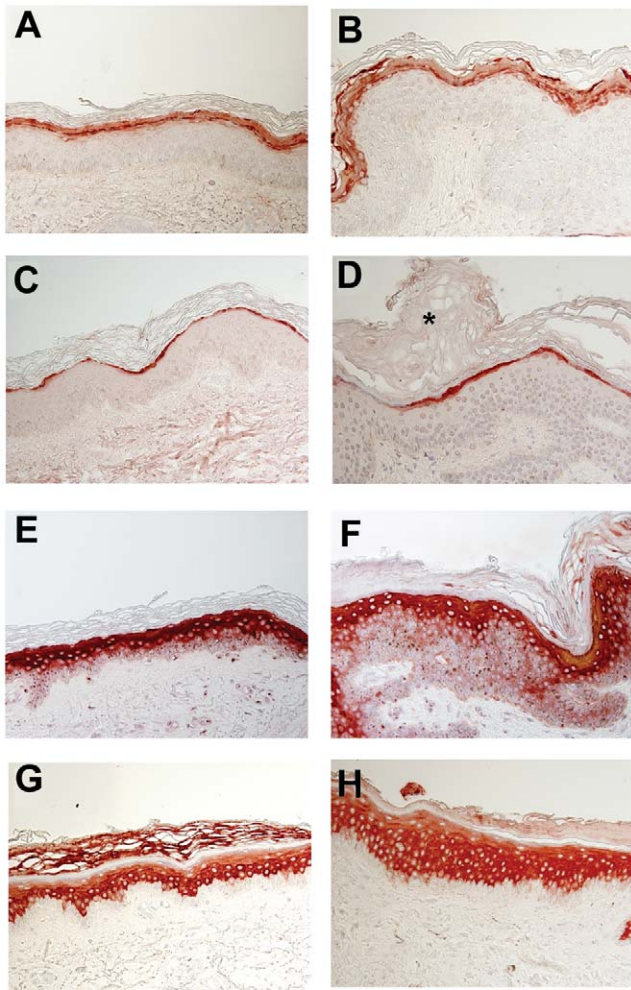


Figure 5. Cornified cell envelope–protein expression (original magnification $\times 400$). Skin-biopsy sections obtained from a control individual (A, C, E, and G) and a patient (B, D, F, and H) were stained with antibodies directed against filaggrin (A and B), loricrin (C and D), involucrin (E and F), and keratin 1 (G and H) and were examined by light microscopy. Note the marked acanthosis (H) and thickened stratum corneum (indicated by an asterisk [*] in panel D) in affected skin.

The present study suggests that matriptase may also be involved in the desquamation process, since degradation of corneodesmosomes in ARIH is impaired. The lack of inhibition of KLK7 and KLK5 by the serine-protease inhibitor LEKTI may be related to the phenotypic manifestations of NTS.³⁸ In NTS, corneodesmosome degradation is accelerated,²⁵ suggesting that matriptase may be an additional substrate for LEKTI. Interestingly, similar to ARIH, the persistence of corneodesmosomes in the stratum corneum was observed in autosomal dominant ichthyosis vulgaris and X-linked ichthyosis.³⁹

No human diseases associated with mutations in the *ST14* gene have been described elsewhere, although matriptase overexpression has been implicated in cancer me-

tastasis.⁴⁰ Matriptase^{-/-}-knockout mice have been generated^{27,41}; these mice die shortly after birth as a result of deficient epidermal-barrier function in the skin in newborns. They also demonstrate abnormal hair-follicle development and disturbed thymic homeostasis that results in increased lymphocyte apoptosis in the thymus of the newborn mice.⁴¹ Our patients did not display any signs suggestive of a T cell–related immunological defect. Interestingly, 3 wk after transplantation of whole skin from matriptase^{-/-} mice to adult athymic nude mice, the skin from the knockout mice showed severe epidermal thickening, the formation of ichthyosislike epidermal scales, and almost complete absence of erupted pelage hairs.⁴² Therefore, systemic expression of matriptase does not correct the epidermal defects in matriptase-deficient skin.

The relatively mild manifestations of ARIH syndrome contrast with the severe phenotype of knockout mice. This may be because the identified missense mutation has a milder effect as compared with total protein deficiency in the knockout mice.

It has been shown that, in mice, matriptase deficiency correlates with abnormal proteolytic processing of the epidermal protein profilaggrin into filaggrin monomer units and the NH₂-terminal filaggrin S-100 regulatory protein, resulting in accumulation of profilaggrin and aberrant profilaggrin-processing products in the stratum corneum.⁴² Although we were unable to directly assess filaggrin processing, the distribution of this protein in the epidermis

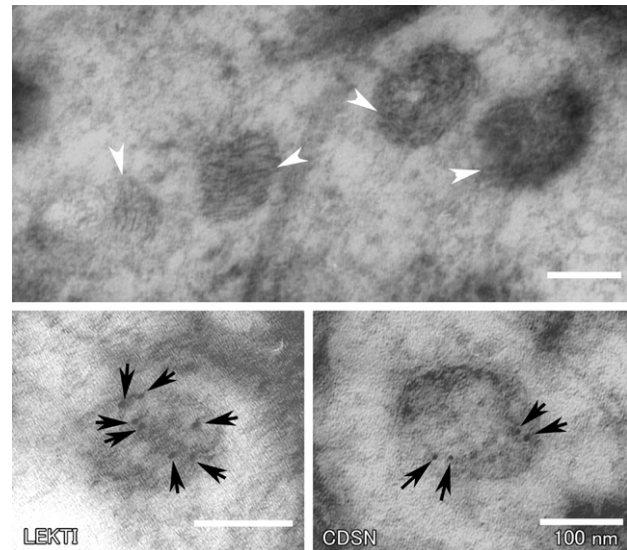


Figure 6. Normal-looking lamellar granules with immunoreactivity to LEKTI and CDSN in the skin of a patient. Skin-biopsy samples from a patient were examined by electron microscopy. The top panel is an unlabeled Lowicryl HM20-embedded section stained with uranyl acetate and lead citrate, showing laminated internal structures within lamellar granules (arrowheads). The lower panels are 5-nm immunogold-labeled (arrows) sections with antibodies against LEKTI and CDSN.

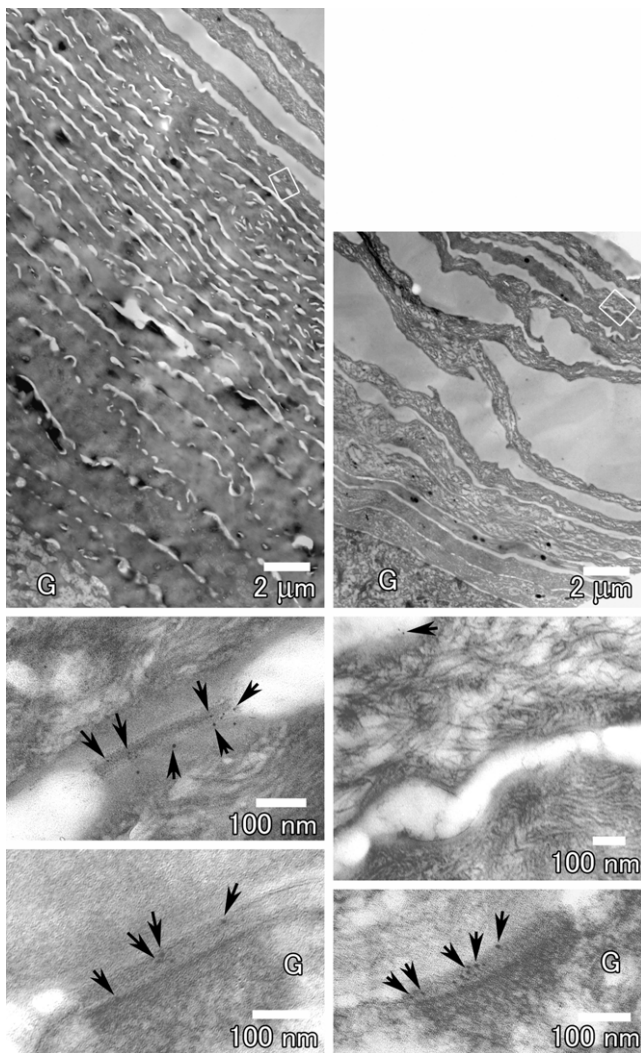


Figure 7. Impaired degradation of corneodesmosomes in affected skin. Skin-biopsy samples from a patient (*left panels*) and a healthy individual (*right panels*) were examined by electron microscopy. Stratum corneum is greatly thickened in the patient's skin compared with that of the control individual (*top panels*, with the same magnification). The rectangular areas marked in the top panels are shown at higher magnifications in the middle panels. Corneodesmosomes are intact in the upper layer, with many CDSN labels (*arrows*) in the patient (*left, middle*), whereas they are degraded with only a few CDSN labels remaining in the upper stratum corneum in normal skin (*right, middle*). The lower panels show desmosomes between the uppermost stratum granulosum (G) and the first cornified cells positively labeled with CDSN in both patient and control skin.

was normal. Ultrastructural analysis of the granular layer of neonatal matriptase^{-/-} epidermis showed sparse and disorganized lamellar bodies. In our patients, lamellar granules were found to be morphologically normal.

All the patients showed various hair abnormalities, including dysplastic hair, pili torti, pili bifurcati, and central pili mono bifurcati. Interestingly, multiple hair abnormal-

ities—including trichorrhexis invaginata, pili torti, trichorrhexis nodosa, and helical hairs—have been reported in NTS.^{43,44}

In conclusion, we have shown that a mutation in *ST14* encoding the type II transmembrane serine protease matriptase causes a novel autosomal recessive genodermatosis characterized by ichthyosis and abnormal hair. The fact that the patients show abnormal degradation of corneodesmosomes in the upper layers of the stratum corneum suggests a role of this protease in epidermal desquamation, possibly via impaired proteolytic degradation of corneodesmosomal proteins.

Acknowledgments

We are grateful to the families who participated in this study. We also thank Dr. G. Halpern for her help with editing the manuscript and Rafi Rainshtein for his help with preparing the figures. We are grateful to Dr. Tamy Shohat for her help with the LOD-score calculation. This study was supported by the Yeshaya Horowitz foundation and in part by a grant provided by the Deutsche Forschungsgemeinschaft (to E.S.).

Web Resources

Accession numbers and URLs for data presented herein are as follows:

BLink, <http://www.ncbi.nlm.nih.gov/sutils/blink.cgi?pid=13124575>

Clustal Alignment, <http://www.hongyu.org/software/clustal.html> (for ClustalW)

ConSeq Server, <http://conseq.bioinfo.tau.ac.il/>

dbSNP, <http://www.ncbi.nlm.nih.gov/SNP/>

Ensembl Genome Browser, <http://www.ensembl.org/>

GenBank, <http://www.ncbi.nlm.nih.gov/Genbank/> (for *Homo sapiens* *ST14*, (accession number NP_068813), prostamin (accession number BAB20376), and serine protease (accession number AAG15395); *P. troglodytes* homologue (accession number XP_508863); *M. musculus* matriptase (accession number BAE38987); *R. norvegicus* matriptase (accession number AAH97271); *G. gallus* matriptase (accession number XP_417872); *C. familiaris* matriptase (accession number XP_546396); *X. laevis* matriptase (accession number AAH71077); and *D. rerio* hypothetical protein (accession number NP_001035441)

Online Mendelian Inheritance in Man (OMIM), <http://www.ncbi.nlm.nih.gov/Omim/> (for *TGM1*; *ALOXE3*; *ALOX12B*; *ABCA12*; *ICHTHYIN*; *FLJ39501*; NTS; congenital ichthyosis, follicular atrophoderma, hypotrichosis, and hypohidrosis syndrome; trichothiodystrophy with congenital ichthyosis; ichthyosis, split hairs, and amino aciduria syndrome; and IFAP syndrome)

Primer3, http://frodo.wi.mit.edu/cgi-bin/primer3/primer3_www.cgi

SIFT, http://blocks.fhcrc.org/sift/SIFT_seq_submit2.html

UCSC Genome Browser, <http://genome.ucsc.edu/>

References

- Huber M, Rettler I, Bernasconi K, Frenk E, Lavrijsen SP, Ponc M, Bon A, Lautenschlager S, Schorderet DE, Hohl D (1995) Mutations of keratinocyte transglutaminase in lamellar ichthyosis. *Science* 267:525–528

2. Russell LJ, DiGiovanna JJ, Rogers GR, Steinert PM, Hashem N, Compton JG, Bale SJ (1995) Mutations in the gene for transglutaminase 1 in autosomal recessive lamellar ichthyosis. *Nat Genet* 9:279–283
3. Kresbsová A, Küster W, Lestringant GG, Schulze B, Hinz B, Frossard PM, Reis A, Hennies HC (2001) Identification, by homozygosity mapping, of a novel locus for autosomal recessive congenital ichthyosis on chromosome 17p, and evidence for further genetic heterogeneity. *Am J Hum Genet* 69: 216–222
4. Jobard F, Lefèvre C, Karaduman A, Blanchet-Bardon C, Emre S, Weissenbach J, Özgüc M, Lathrop M, Prud'homme J-F, Fischer J (2002) Lipoxygenase-3 (*ALOXE3*) and 12 (*R*)-lipoxygenase (*ALOX12B*) are mutated in non-bullous congenital ichthyosiform erythroderma (NCIE) linked to chromosome 17p13.1. *Hum Mol Genet* 11:107–113
5. Lefèvre C, Audebert S, Jobard F, Bouadjar B, Lakhdar H, Boughdene-Stambouli O, Blanchet-Bardon C, Heilig R, Foglio M, Weissenbach J, et al (2003) Mutations in the transporter *ABCA12* are associated with lamellar ichthyosis type 2. *Hum Mol Genet* 12:2369–2378
6. Kelsell DP, Norgett EE, Unsworth H, Teh M-T, Cullup T, Mein CA, Dopping-Hepenstal PJ, Dale BA, Tadini G, Fleckman P, et al (2005) Mutations in *ABCA12* underlie the severe congenital skin disease Harlequin ichthyosis. *Am J Hum Genet* 76:794–803
7. Lefèvre C, Bouadjar B, Karaduman A, Lefevre C, Bouadjar B, Karaduman A, Jobard F, Saker S, Özgüc M, Lathrop M, et al (2004) Mutations in *ichthyin* a new gene on chromosome 5q33 in a new form of autosomal recessive congenital ichthyosis. *Hum Mol Genet* 13:2473–2482
8. Lefèvre C, Bouadjar B, Ferrand V, Tadini G, Megarbane A, Lathrop M, Prud'homme JF, Fischer J (2006) Mutations in a new cytochrome P450 gene in lamellar ichthyosis type 3. *Hum Mol Genet* 15:767–776
9. Mizrachi-Koren M, Geiger D, Indelman M, Bitterman-Deutsch O, Bergman R, Sprecher E (2005) Identification of a novel locus associated with congenital recessive ichthyosis on 12p11.2-q13. *J Invest Dermatol* 125:456–462
10. Virolainen E, Wessman M, Hovatta I, Niemi K-M, Ignatius J, Kere J, Peltonen L, Palotie A (2000) Assignment of a novel locus for autosomal recessive congenital ichthyosis to chromosome 19p13.1-p13.2. *Am J Hum Genet* 66:1132–1137
11. Sprecher E (2005) Genetic hair and nail disorders. *Clin Dermatol* 23:47–55
12. Chavanas S, Bodemer C, Rochat A, Hamel-Teillac D, Ali M, Irvine AD, Bonafe JL, Wilkinson J, Taieb A, Barrandon Y, et al (2000) Mutations in *SPINK5*, encoding a serine protease inhibitor, cause Netherton syndrome. *Nat Genet* 25:141–142
13. Lestringant GG, Kuster W, Frossard PM, Happel R (1998) Congenital ichthyosis, follicular atrophoderma, hypotrichosis, and hypohidrosis: a new genodermatosis? *Am J Med Genet* 75: 186–189
14. Tursen U, Kaya TI, Ikizoglu G, Aktekin M, Aras N (2002) Genetic syndrome with ichthyosis: congenital ichthyosis, follicular atrophoderma, hypotrichosis, and woolly hair: second report. *Brit J Derm* 147:604–631
15. Weeda G, Eveno E, Donker I, Vermeulen W, Chevallier-Lagente O, Taieb A, Sary A, Hoeijmakers JHJ, Mezzina M, Sarasin A (1997) A mutation in the *XPB/ERCC3* DNA repair transcription gene, associated with trichothiodystrophy. *Am J Hum Genet* 60:320–329
16. Broughton BC, Berneburg M, Fawcett H, Taylor EM, Arlett CE, Nardo T, Stefanini M, Menefee E, Price VH, Queille S, et al (2001) Two individuals with features of both xeroderma pigmentosum and trichothiodystrophy highlight the complexity of the clinical outcomes of mutations in the *XPB* gene. *Hum Molec Genet* 10:2539–2547
17. Yesudian P, Srinivas K (1977) Ichthyosis with unusual hair shaft abnormalities in siblings. *Brit J Derm* 96:199–203
18. Sambrook J, Fritsch EF, Maniatis T (1987) *Molecular cloning: a laboratory manual*. Cold Spring Harbor Laboratory, Cold Spring Harbor, NY
19. Fishelson M, Geiger D (2002) Exact genetic linkage computations for general pedigrees. *Bioinformatics Suppl* 18:S189–S198
20. Higgins D, Thompson J, Gibson T (1994) CLUSTAL W: improving the sensitivity of progressive multiple sequence alignment through sequence weighting, position-specific gap penalties and weight matrix choice. *Nucleic Acids Res* 22:4673–4680
21. Clamp M, Cuff J, Searle SM, Barton GJ (2004) The Jalview Java alignment editor. *Bioinformatics* 20:426–427
22. Berezin C, Glaser F, Rosenberg J, Paz I, Pupko T, Fariselli P, Casadio R, Ben-Tal N (2004) ConSeq: the identification of functionally and structurally important residues in protein sequences. *Bioinformatics* 20:1322–1324
23. Ng PC, Henikoff S (2002) Accounting for human polymorphisms predicted to affect protein function. *Genome Res* 12: 436–446
24. Ishida-Yamamoto A, Simon M, Kishibe M, Miyauchi Y, Takahashi H, Yoshida S, O'Brien TJ, Serre G, Iizuka H (2004) Epidermal lamellar granules transport different cargoes as distinct aggregates. *J Invest Dermatol* 122:1137–1144
25. Descargues P, Deraison C, Bonnart C, Kreft M, Kishibe M, Ishida-Yamamoto A, Elias P, Barrandon Y, Zambruno G, Sonnenberg A, et al (2005) *Spink5*-deficient mice mimic Netherton syndrome through degradation of desmoglein 1 by epidermal protease hyperactivity. *Nat Genet* 37:56–65
26. Olson LE, Zhang J, Taylor H, Rose DW, Rosenfeld MG (2005) *Barx2* functions through distinct corepressor classes to regulate hair follicle remodeling. *Proc Natl Acad Sci USA* 102: 3708–3713
27. List K, Bugge TH, Szabo R (2006) Matriptase: potent proteolysis on the cell surface. *Mol Med* 12:1–7
28. König A, Happel R (1999) Linear lesions reflecting lyonization in women heterozygous for IFAP syndrome (ichthyosis follicularis with atrichia and photophobia). *Am J Med Genet* 85:365–368
29. Hooper JD, Clements JA, Quigley JP, Antalis TM (2001) Type II transmembrane serine proteases: insights into an emerging class of cell surface proteolytic enzymes. *J Biol Chem* 276: 857–860
30. Lin CY, Anders J, Johnson M, Sang QA, Dickson RB (1999) Molecular cloning of cDNA for matriptase, a matrix-degrading serine protease with trypsin-like activity. *J Biol Chem* 274: 18231–18236
31. Oberst MD, Singh B, Ozdemirli M, Dickson RB, Johnson MD, Lin CY (2003) Characterization of matriptase expression in normal human tissues. *J Histochem Cytochem* 51:1017–1025
32. List K, Szabo R, Molinolo A, Nielsen BS, Bugge TH (2006) Delineation of matriptase protein expression by enzymatic gene trapping suggests diverging roles in barrier function, hair

- formation, and squamous cell carcinogenesis. *Am J Pathol* 168:1513–1512
33. Lin CY, Wang JK, Torri J, Dou L, Sang QA, Dickson RB (1997) Characterization of a novel, membrane-bound, 80-kDa matrix-degrading protease from human breast cancer cells: monoclonal antibody production, isolation, and localization. *J Biol Chem* 272:9147–9152
 34. Cho EG, Kim MG, Kim C, Kim SR, Seong IS, Chung C, Schwartz RH, Park D (2001) N-terminal processing is essential for release of epithin, a mouse type II membrane serine protease. *J Biol Chem* 276:44581–44589
 35. Oberst MD, Williams CA, Dickson RB, Johnson MD, Lin CY (2003) The activation of matriptase requires its noncatalytic domains, serine protease domain, and its cognate inhibitor. *J Biol Chem* 278:26773–26779
 36. Zeeuwen P (2004) Epidermal differentiation: the role of proteases and their inhibitors. *Eur J Cell Biol* 83:761–773
 37. Caubet C, Jonca N, Brattsand M, Guerrin M, Bernard D, Schmidt R, Egelrud T, Simon M, Serre G (2004) Degradation of corneodesmosome proteins by two serine proteases of the kallikrein family, SCTE/KLK5/hK5 and SCCE/KLK7/hK7. *J Invest Dermatol* 122:1235–1244
 38. Egelrud T, Brattsand M, Kreutzmann P, Walden M, Vitzthum K, Marx UC, Forssmann WG, Magert HJ (2005) hK5 and hK7, two serine proteinases abundant in human skin, are inhibited by LEKTI domain 6. *Br J Dermatol* 153:1200–1203
 39. Elsayed-Ali H, Barton S, Marks R (1992) Stereological studies of desmosomes in ichthyosis vulgaris. *Br J Dermatol* 126:24–28
 40. Satomi S, Yamasaki Y, Tsuzuki S, Hitomi Y, Iwanaga T, Fushiki T (2001) A role for membrane-type serine protease (MT-SP1) in intestinal epithelial turnover. *Biochem Biophys Res Commun* 287:995–1002
 41. List K, Haudenschild CC, Szabo R, Chen W, Wahl SM, Swaim W, Engelholm LH, Behrendt N, Bugge TH (2002) Matriptase/MT-SP1 is required for postnatal survival, epidermal barrier function, hair follicle development, and thymic homeostasis. *Oncogene* 21:3765–3779
 42. List K, Szabo R, Wertz PW, Segre J, Haudenschild CC, Kim SY, Bugge TH (2003) Loss of proteolytically processed filaggrin caused by epidermal deletion of matriptase/MT-SP1. *J Cell Biol* 163:901–910
 43. Ito M, Ito K, Hashimoto K (1984) Pathogenesis in trichorrhexis invaginata (bamboo hair). *J Invest Dermatol* 83:1–6
 44. Lurie R, Garty BZ (1995) Helical hairs: a new hair anomaly in a patient with Netherton's syndrome. *Cutis* 55:349–352